ELSEVIER

Surface Science 441 (1999) 107–116

surface science

www.elsevier.nl/locate/susc

Surface structures of S on Pd(111)

S. Speller [a], T. Rauch [a], J. Bömermann [a], P. Borrmann [b], W. Heiland [a,*]

[a] *Fachbereich Physik, Universität Osnabrück, 49069 Osnabrück, Germany*
[b] *Fachbereich Physik, Universität Oldenburg, 26111 Oldenburg, Germany*

Received 26 May 1999; accepted for publication 13 July 1999

Abstract

S is adsorbed on Pd(111) from the gas phase using H_2S as 'carrier' gas. After adsorption at room temperature a $(\sqrt{3}\times\sqrt{3})R30^\circ$ LEED pattern is observed. Using STM coexisting $(\sqrt{3}\times\sqrt{3})R30^\circ$, $(\sqrt{7}\times\sqrt{7})R19.1^\circ$ (2×2) stripes, (2×2) triangles and disordered S structures are found. Annealing favors the formation of $(\sqrt{7}\times\sqrt{7})R19.1^\circ$ areas on the surface. The structures, produced by H_2S adsorption are compared with S structures produced by segregation. A detailed model for the $(\sqrt{7}\times\sqrt{7})R19.1^\circ$ is developed on the basis of AES and XPS data and FLAPW calculations.

Keywords: Low energy electron diffraction (LEED); Chemisorption; Palladium; Scanning tunneling microscopy; Sulfur; Surface segregation; Surface structure, morphology, roughness, and topography; X-ray photoelectron spectroscopy

1. Introduction

Interest in the Pd surface is due to the catalytic properties of this metal, naturally, with many other catalytically active metals in neighboring positions in the periodic table. S on Pd(111) plays a role in the formation of thiophene, C_4H_4S, from acetylene C_2H_2, which is a cyclization reaction [1]. The clean Pd(111) surface is known to promote the cyclization of acetylene to benzene [2,3]. Previous studies on the adsorption of S on Pd(111) used H_2S [1,4–6], S_2 [7] or surface segregation of S [8,9].

In the gas adsorption studies a $(\sqrt{3}\times\sqrt{3})R30^\circ$ is found by low energy electron diffraction (LEED) and scanning tunneling microscopy (STM) which converts into a $(\sqrt{7}\times\sqrt{7})R19.1^\circ$ structure during heating to above 370 K. For segregation, temperatures of approximately 700 K are needed to produce an S coverage of 0.20 monolayers determined by AES. The predominant LEED pattern is then $(\sqrt{7}\times\sqrt{7})R19.1^\circ$. Using STM, however, areas containing disordered S, (2×2) triangular two-dimensional (2D) S islands and (2×2) S stripes decorating the steps of the Pd(111) surface are also found. The adsorption site of S in the $(\sqrt{3}\times\sqrt{3})R30^\circ$ pattern was identified as the three-fold fcc site in agreement with the previous LEED analysis [5]. Recently the $(\sqrt{7}\times\sqrt{7})R19.1^\circ$ structure was reanalyzed by TLEED (Tensor-LEED) [10] which led to a new reconstruction model. In the present study we used H_2S adsorption in order make a comparison with the segregation study [8,9] and to get a basis of comparison with previous work [1,4–7,10].

2. Experiment

For the experiments we use an Omicron STMI instrument which is equipped with a scanning

* Corresponding author. Fax: +49 541 969 2670.
E-mail address: wheiland@uos.de (W. Heiland)

0039-6028/99/$ – see front matter
PII: S0039-6028(99)00808-0

tunneling microscope, an analysis chamber and a preparation chamber. The analysis and the STM chamber share a vacuum of 5×10^{-11} mbar. The analysis chamber is equipped for Auger electron spectroscopy (AES), X-ray photoelectron spectroscopy (XPS), reflection high energy electron diffraction (RHEED) and LEED. For the present study we did not use RHEED. After surface analysis the sample is transferred quickly (in less than 1 min) to the STM using a wobble stick. The three fine piezo elements of the STM have been calibrated using the Si(111)(7×7) and the Pt(110)(1×2) surface superstructures and step heights. All STM images are taken at room temperature. The preparation chamber is at a base pressure of 1×10^{-10} mbar. Here, sputtering and annealing of the samples, as well as the exposure to H_2S gas, are carried out. We report here results from exposure to a saturation coverage only. The surface becomes inert after adsorption of approximately one layer of S, i.e. we found only very few and small patches with multilayer adsorption. Before sputtering, the sample was annealed to 750 K in order to remove H which can be incorporated within the surface region after the dissociation of the H_2S molecules on the surface. The annealing temperature for the Pd(111) surface was chosen clearly below the temperature for segregation of 700 K. Further details about the instrument and the surface preparation are described in Ref. [11].

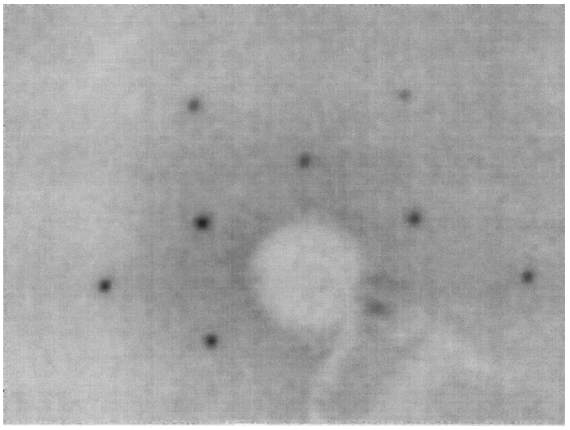

Fig. 1. $(\sqrt{3}\times\sqrt{3})$R30° LEED pattern from a Pd(111) surface after exposure to H_2S.

3. Results

When exposing the Pd(111) surface at 10^{-7} mbar for 2 min to H_2S at room temperature we observe the LEED $(\sqrt{3}\times\sqrt{3})$R30° (Fig. 1)

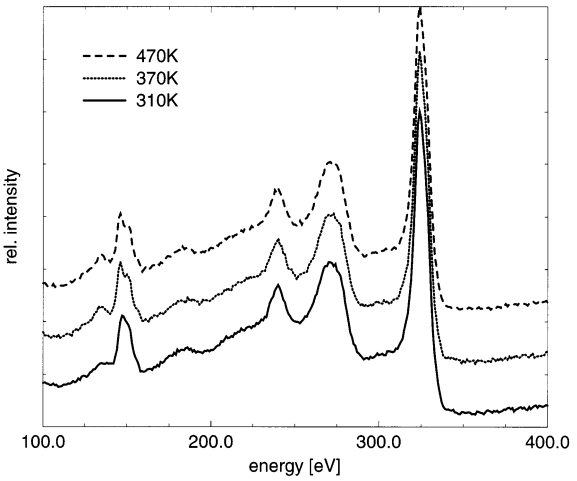

Fig. 2. AES spectra from an S-covered Pd(111) surface after the exposure at room temperature and after annealing to 370 and 470 K respectively. The peaks at approximately 150 eV are from S, all other peaks are from Pd.

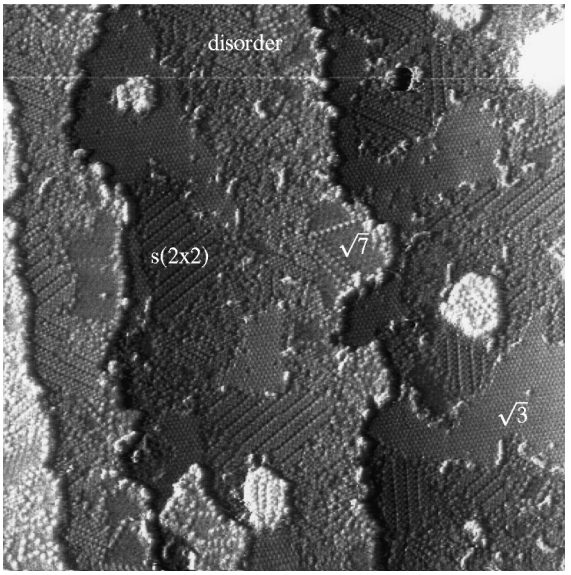

Fig. 3. STM overview (640 Å × 640 Å) of the S-covered Pd(111) surface after exposure to H_2S. Visible are disordered, $(\sqrt{3}\times\sqrt{3})$R30°, $(\sqrt{7}\times\sqrt{7})$R19.1° and s(2×2) areas.

pattern as reported by other groups [1,4–7]. The coverage corresponding to the AES spectrum (Fig. 2), evaluated after differentiation by the standard peak-to-peak height method, is 0.22 monolayer (see also Table 2), where one monolayer is defined as an S layer with the Pd(111) surface lattice constant. We measured the S surface concentration also by XPS. The AES and XPS results will be considered in detail in Section 4. Using STM a rather large variety of different structures is observed after exposure to H_2S gas. Fig. 3 shows a typical STM image of the surface topography. In detail we observe the following structures. In the upper middle region of Fig. 3 a disordered area is visible. We call areas 'disordered' when no periodic structure is obvious. In the disordered areas changes are found from scan to scan indicating S mobility at room temperature. Additionally, different types of ordered patches are visible: exemplary in Fig. 3 one area of each observed structure is labeled. The largest ordered patches are $(\sqrt{3}\times\sqrt{3})R30^\circ$ structures as revealed when zooming into one of those areas (Fig. 4a). The relatively low occurrence of the $(\sqrt{3}\times\sqrt{3})R30^\circ$ of approximately 25% is obvious already when inspecting the STM images by eye. Movies from $(\sqrt{3}\times\sqrt{3})R30^\circ$ areas revealed that the vacancies (four of them are present in Fig. 4a) jump around with time. An effect from the force of the tip cannot be excluded completely, although such mobility has not been observed in the other ordered S structures. Fig. 4b shows a model of the $(\sqrt{3}\times\sqrt{3})R30^\circ$ structure in agreement with all previous reports of this structure [1,4–7]. The structure of the stripes is (2×2);

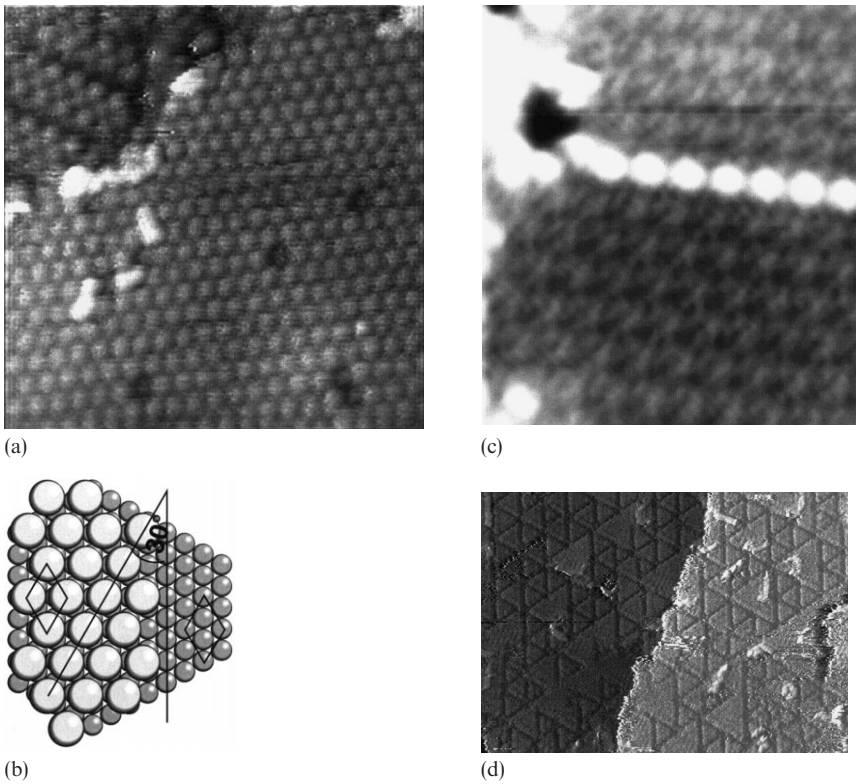

Fig. 4. (a) STM topograph (100 Å × 100 Å) of a $(\sqrt{3}\times\sqrt{3})R30^\circ$ area bordered by a s(2×2) area (upper left). Note the 'roughness' of the step. The distance between adjacent white spots, S, is 5.1 Å in satisfactory agreement with the $(\sqrt{3}\times\sqrt{3})R30^\circ$ structure. (b) Model of the $(\sqrt{3}\times\sqrt{3})R30^\circ$ structure. (c) STM topograph (80 Å × 80 Å) of a $(\sqrt{7}\times\sqrt{7})R19.1^\circ$ area with two domains. The domain boundary is decorated by the almost horizontal chain of bright objects. (d) STM topograph (360 Å × 250 Å) of an adsorption area with triangular 2D islands in a (2×2) pattern. These are rare features in the case of H_2S exposure.

we call them stripe, 's(2×2)', structures (Fig. 4a, upper left hand corner). The stripes have a width of two to four atoms. They are separated by dark lines. These are domain boundaries. Neighboring stripe structures are shifted with respect to each other by one [110] lattice unit. There are also a few 'elevated', white islands (Fig. 3) which are possibly due to double S-layering. This structure is not clearly identified. These features are rather rare when exploring larger areas of the surface. Finally there is the patch, approximately in the middle, characterized by 'white dotted' lines. This is a $(\sqrt{7}\times\sqrt{7})$R19.1° structure (see also Fig. 4c). The white lines separate two $(\sqrt{7}\times\sqrt{7})$R19.1° translation domains in which the S adsorption sites are shifted with respect to each other by 4.8 Å ($2a_1\cos 30°$ where a_1 is the nearest neighbor distance of Pd) in this case. In general, there exist two rotation domains each inhering seven translation domains. This feature has also been seen in the case of the $(\sqrt{7}\times\sqrt{7})$R19.1° structure prepared by segregation [8,9]. We determined the lattice constants of the clean Pd and the S superstructures by a Fourier transformation of sections along atomic rows. Usually the substrate and the S film cannot be resolved atomically simultaneously.

After the room temperature adsorption there are only a few areas of triangularly shaped S islands (Fig. 4d) not appearing in the overview image of Fig. 3. The triangles contain approximately 70 S atoms on average. The structure of these S islands or 2D clusters is (2×2). These

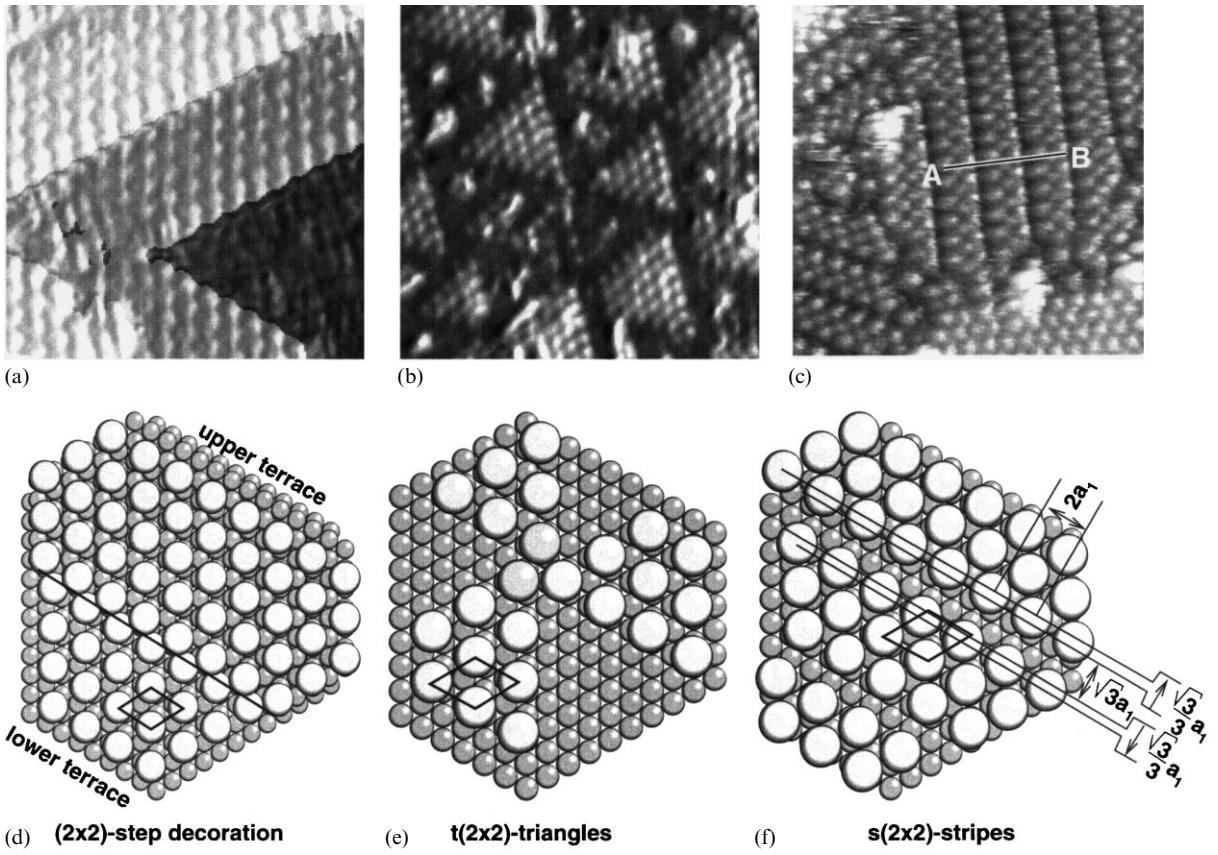

Fig. 5. STM topographs and models of the three types of (2×2) S structure. (a) Steps on Pd(111) after S segregation (80 Å × 80 Å). (b) 2D triangular S islands produced by segregation (120 Å × 120 Å). (c) Bands formed after S adsorption (90 Å × 90 Å). (d–f) Models of the (2×2) structures of a–c.

islands are rare in the adsorption study. In contrast, triangular islands, 't(2×2)', are formed copiously in the case of segregation (Fig. 5b) [8,9]. Another interesting difference of adsorption versus segregation is the different structure of the steps of the Pd surface. In the segregation case the steps are decorated by a rim of s(2×2) S rows, three to four atoms wide, and well defined (Fig. 5a). However, in case of gas phase adsorption, the steps are irregular without any straight sections. The features of the H_2S adsorption-induced topographies are well reproduced in the sense that the disordered, the s(2×2) (Fig. 5c), the $(\sqrt{3}\times\sqrt{3})$R30° and the $(\sqrt{7}\times\sqrt{7})$R19.1° areas are always observed. However the relative occurrences of these features vary for different preparations. In Fig. 5d–f we show models of the different (2×2) structures.

When heating the crystal with exposures initially leading to the $(\sqrt{3}\times\sqrt{3})$R30° LEED pattern and STM topographies as in Fig. 3 to temperatures above approximately 370 K the LEED pattern changes to $(\sqrt{7}\times\sqrt{7})$R19.1° (Fig. 6) as reported previously [1,4–7]. The LEED pattern is a superposition of two types of S $(\sqrt{7}\times\sqrt{7})$R19.1° domains rotated by + and −19.1° with respect to the Pd(111) lattice. The LEED patterns of the S film after adsorption and anneal are qualitatively 'better' than those observed after S segregation [8,9]. These may be caused by the higher occurrence of the $(\sqrt{7}\times\sqrt{7})$R19.1° structure in the case of H_2S adsorption (up to 90% after anneal), compared with the segregation case, where the $(\sqrt{7}\times\sqrt{7})$R19.1° structure competes with the triangular (2×2) structure and covers therefore less area. In the AES data we observe a splitting of the S(LMM) peak at 152 eV S peak (Fig. 2). The annealing changes slightly the S peak shape and area. The qualitative change of the LEED pattern from $(\sqrt{3}\times\sqrt{3})$R30° to $(\sqrt{7}\times\sqrt{7})$R19.1° is achieved after a 370 K anneal. Using STM a general decrease of the disordered areas in favor of the $(\sqrt{3}\times\sqrt{3})$R30° and with a preference of the $(\sqrt{7}\times\sqrt{7})$R19.1° areas is observed, but there are always a few s(2×2) stripes left. Further heating to above 370 K causes a significant growth of the $(\sqrt{7}\times\sqrt{7})$R19.1° areas and a decrease of the $(\sqrt{3}\times\sqrt{3})$R30° and the s(2×2) areas (Fig. 7). Heating to higher temperatures, up to 700 K, does not change this general behavior. There is no evidence for S segregation on the S-covered Pd(111) surface as in case of the clean Pd(111) surface, i.e. the S coverage of the pre-covered surface does not increase when the surface is kept at temperature and for times long enough to cause segregation on the clean surface. H_2S adsorption at elevated temperature leads to results equivalent to the ones obtained via room temperature adsorption followed by heating.

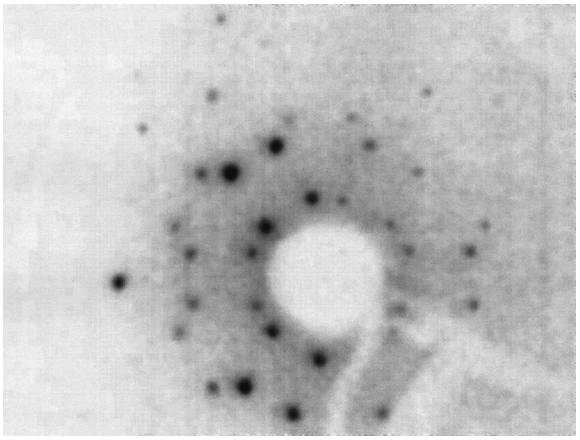

Fig. 6. LEED pattern $(\sqrt{7}\times\sqrt{7})$R19.1° after annealing to 400 K for the same coverage as in Fig. 1.

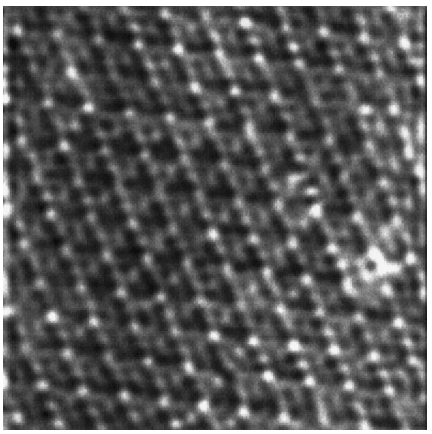

Fig. 7. STM overview of a $(\sqrt{7}\times\sqrt{7})$R19.1° (80 Å × 80 Å) after annealing to 470 K of a Pd(111) surface exposed to H_2S. In order to make the atoms in between the $(\sqrt{7}\times\sqrt{7})$R19.1° S atoms visible this image has been Fourier filtered.

Table 1
S-induced structures observed on Pd(111). s refers to stripes and t refers to triangles. The first two columns on the left list the coverage (Θ) and the nearest neighbor distance (nnd) of each S structure. Preparation temperatures are on purpose not given, since they do not result in one homogenous phase, but change only the relative occurrences of the phases

Θ	nnd (Å)	Structure	Ref. [1]	Ref. [4]	Ref. [6]	Ref. [7]	Ref. [8,9]	This work
0.14	7.3	$(\sqrt{7}\times\sqrt{7})$R19.1°[a]	yes	yes	yes	yes	yes	yes
0.25	5.5	s(2×2)[b]	no	no	no	no	yes	yes
0.25	5.5	t(2×2)[c]	no	no	no	no	yes	yes
0.33	4.8	$(\sqrt{3}\times\sqrt{3})$R30°	yes	yes	yes	yes	no	yes

[a] Here we give values for the simple $(\sqrt{7}\times\sqrt{7})$R19.1° structure when only one S atom is in the unit mesh.
[b] The s(2×2) structure is found exclusively at steps after segregation and only on terraces after S adsorption.
[c] After segregation also (6×6) structures have been observed, which are a degenerated form of the t(2×2) structure. The triangles consist of three atoms only and their arrangement is in (6×6) periodicity [11].

4. Discussion

In Table 1 we summarize the results of our H_2S adsorption experiments, together with those of previous work on the Pd(111)+S system. In our studies the nearest neighbor distances (nnd) are derived from the respective patterns in STM images. For the $(\sqrt{7}\times\sqrt{7})$R19.1° structure we took only the largest white features into account, keeping in mind that the actual coverage is rather 2/7 monolayers and even 3/7 monolayers in the other studies [1,4,6]. From nnd in turn the coverage Θ is calculated.

Annealing to above 370 K is necessary to grow large areas of the $(\sqrt{7}\times\sqrt{7})$R19.1° structure. In doing so, the relative occurrence of the other structures decreases. With the annealing process we observe a slight decrease of the S coverage in AES.

It is obvious that in work based on LEED for structural analysis the (2×2) features are not found. In both the segregation study and our present work we find all four structures with STM, albeit the LEED shows either $(\sqrt{3}\times\sqrt{3})$R30° or $(\sqrt{7}\times\sqrt{7})$R19.1° pattern. In some details the S segregation and the H_2S adsorption lead to differences, i.e. the segregated S decorates the steps with s(2×2) stripes whereas the H_2S adsorption leads to extended fields of s(2×2) stripes on the terraces. We note that the stripes show contraction (in Fig. 5c hard to be seen) when a large number of the stripes is analyzed, i.e. the edge atoms are apparently moved towards the center of the stripes by approximately 1.6 Å or $\sqrt{3}a_1/3$ where a_1 is the nearest neighbor Pd distance (Fig. 5f). This type of stripe has not been seen before on fcc(111) surfaces. Stripes of a different nature are rather common on fcc(110) surfaces after adsorption of O [12–14]. For the understanding of the phenomenon lateral surface stress has been invoked [12]. The fact that after segregation the dense (2×2) structure is found only at the steps and in their vicinity could be due to stronger segregation at steps. Also the atoms at steps can generally relax more than atoms in a terrace. The triangular shaped 2D islands are not recognizable by LEED naturally, owing to the lack of long-range order.

The reason for the presence of acute angles only (and the absolute absence of obtuse angles) as found at the S triangles and the (2×2) S bands at steps segregation can be directly assigned to the even valence of S, since obtuse angles at the border of 2D S structures would force the atoms at the border to form odd bonds. For the formation of the triangular islands during segregation a statistical model has been developed which describes the essential properties of the effect. The main requirement of the model is that each S atom prefers to form as many even bonds as possible with other S atoms and to avoid bond breaking. Initially 0.25 ML S are distributed randomly on a 500 Å^2 large area with a hexagonal lattice (periodic boundary conditions). The influence of the Pd(111) substrate is neglected apart from its hexagonal structure. The S atoms undergo a random walk as long as they are single atoms. With an

increasing number of bonds or neighbors they become immobilized naturally. A computer simulation of the random walk taking into account decreasing probability of breaking off when more bonds are formed reproduces the triangular shaped islands (Fig. 8). The size is limited because of the statistics of the initial starting positions for each island. The calculation shows both orientations of the islands. After segregation only one orientation of the triangles is observed.

A second model calculation was used in order to estimate the optimal size of the triangles. Here, the S atoms are held in their sites (in a hexagonal 2D lattice) by an attractive potential (harmonic oscillator). The interaction of neighboring atoms is modelled by a Lennard-Jones potential. Hence the potential energy of the S atoms is:

$$V=\sum_{i=1}^{N}(x_i-xg_i)^2+\frac{1}{2}\sum_{i=1}^{N}\sum_{j=\text{neighbor}}U(r_{ij}),$$

with

$$U=4\epsilon\left[\frac{1}{4}\left(\frac{\sigma}{r}\right)^{12}-\frac{1}{2}\left(\frac{\sigma}{r}\right)^{6}\right].$$

The xg_i are the coordinates of the lattice sites (lattice parameter = 1). The parameter ϵ is arbitrarily used to fit the potential. The minimum of U is at σ. When the S atoms stay at the default sites ($\sigma \approx 1$) the optimal island size is at ∞. Finite island sizes become favorable when the distance between S atoms exceeds clearly the default of the hexagonal substrate lattice ($\sigma \geq 1.2$). The optimal edge length corresponds then to 10 atoms in acceptable agreement with the experiment. Using STM, however, no deviation from the (2×2) period has been found in the triangles. Therefore, the limited island size seems rather to result from the antiphase relation of the $t(2\times2)$ structures in neighboring triangles, which is frequently observed experimentally.

In the STM topographies the dark lines between the triangles are domain boundaries (Fig. 5b and e). In the case of the segregation larger areas of $t(2\times2)$ are found in comparison with $(\sqrt{7}\times\sqrt{7})$R19.1° areas, whereas starting from adsorption the $(\sqrt{3}\times\sqrt{3})$R30°, $s(2\times2)$ and $(\sqrt{7}\times\sqrt{7})$R19.1° structure dominate and $t(2\times2)$ is a rather rare feature. This effect of island formation, although rectangular in shape, has been found for S on Pd(100) by STM [15]. There, S is seen as white spots as in our case.

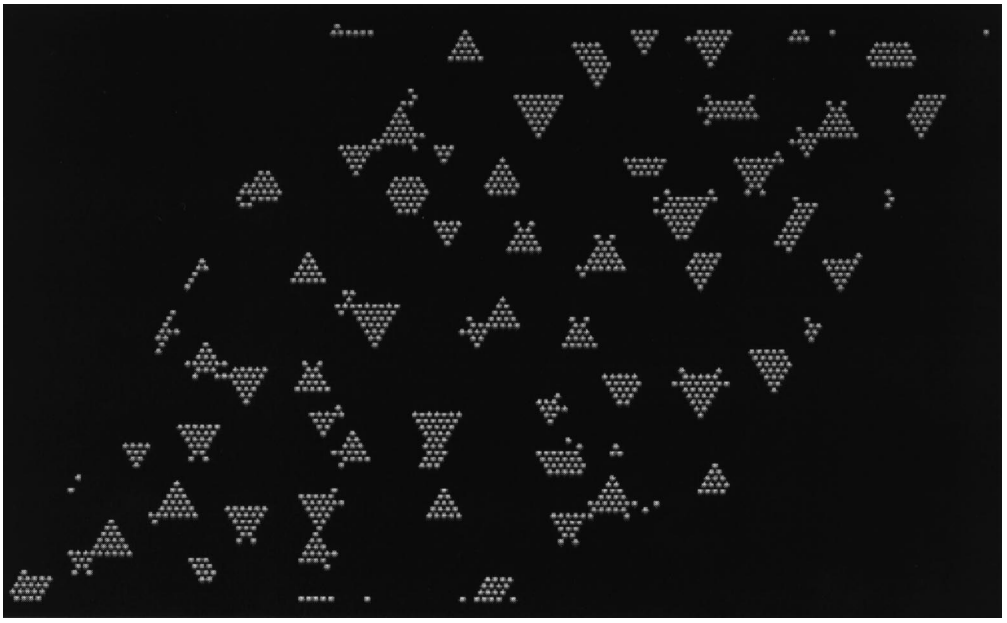

Fig. 8. 'Snapshot' from the simulation (200 Å × 200 Å) of the 2D triangular S islands produced by segregation.

The authors of Ref. [15] put forward an explanation starting from a different point of view from that of our model. They argue that S occupies preferentially sites with the highest available coordination number. Furthermore S is electronegative on metals and, hence, there is a short-range repulsion between S atoms. The growth of larger domains is inhibited by potential barriers which S atoms would have to cross when hopping to a vacancy site in a neighboring island. The latter argument would also support formation of triangular islands on Pd(111).

In Fig. 5d–e we present models of the three (2×2) structures found in the adsorption and segregation studies. The decoration of steps (Fig. 5a and d) and the triangular clusters (Fig. 5b and e) are observed after segregation only. We assume fcc sites for the S atoms in these models, as is the case of the $(\sqrt{3}\times\sqrt{3})$R30° structure [5] . Fig. 5f is a model of the s(2×2) stripes. Here the shift of the rows by $\sqrt{3}a_1/3$ is demonstrated which was evaluated from the STM topographs. $2a_1$ is the lattice constant of the regular (2×2) structure on Pd(111), a_1 is the nearest neighbor distance of Pd or the atom–atom distance of the $\langle 1\bar{1}0\rangle$ rows. The S rows of the (2×2) S stripes are shifted by a_1 with respect to the rows of the neighboring stripes. Without a detailed theoretical modeling it is speculative how and why the s(2×2) stripes are formed, and why they are formed during S adsorption and not on the terraces by segregation.

We agree with Ref. [15] that the white spots on Pd(100) and in the (2×2) structures on Pd(111) are very likely S atoms. This identification is also based on previous theoretical work [16–18]. We expand the conclusion, that S atoms in an adlayer are 'white', to the white spots of the $(\sqrt{7}\times\sqrt{7})$R19.1° structure. The argument does not include the higher lines of atoms (white dotted lines) decorating the domain boundaries of the $(\sqrt{7}\times\sqrt{7})$R19.1° structure. The domains are shifted with respect to each other by 4.8 Å. Also boundaries between the reflection domains are separated by one or more of the same type of dotted lines. Note that t(2×2) and s(2×2) domains, when shifted with respect to each other, have 'dark' boundaries. In Fig. 7 we show an overview STM image of the $(\sqrt{7}\times\sqrt{7})$R19.1° structure.

For modeling the $(\sqrt{7}\times\sqrt{7})$R19.1° structure the number of S atoms in the surface unit cell is decisive. With one S atom per unit cell, equivalent to a coverage of 0.14 monolayers, a simple model was proposed with S atoms on fcc sites [8,9]. Note that in the $(\sqrt{3}\times\sqrt{3})$R30° structure the S atoms occupy fcc sites [5]. In the present work using H_2S adsorption we obtain higher coverages of approximately 0.28 monolayers for the $(\sqrt{7}\times\sqrt{7})$R19.1° structure. This coverage is close to 2/7 allowing two S atoms in the unit cell.

The S coverage has been measured by AES (Fig. 2) and XPS. The results are summarized in Table 2. The values are given for a situation like that in the STM topograph given in Fig. 3 (patched layer) and for an annealed $(\sqrt{7}\times\sqrt{7})$R19.1° structure, for which the STM topographies shows a relative occurrence of $(\sqrt{7}\times\sqrt{7})$R19.1° of approximately 0.90. The relative coverage cannot be measured precisely by STM, because it is impossible to measure the whole area seen by the electron energy analyzer in AES or XPS. The coverage data obtained by both methods depend critically in whether it is assumed that the S is adsorbed in a layer *on* the surface or is distributed homogeneously *in* the surface layer within the range of the emitted electrons. Other details of the evaluation, e.g. the treatment of the background, cause changes within the error bars representing the statistical errors only. In cases of AES we used

Table 2
Concentration of a monolayer of S on Pd evaluated from AES and XPS by different methods (see text) for a patched layer (p.l.) as e.g. in Fig. 3 and for the $(\sqrt{7}\times\sqrt{7})$R19.1° structure. P = peak-to-peak, B = peak to background, L = single layer, A = peak area, T = Tougaard background method

Method	Evaluation	p.l. (%)	$(\sqrt{7}\times\sqrt{7})$R19.1° (%)
AES	d$N(E)$/dE P	22 ± 2	19 ± 2
	d$N(E)$/dE B	20 ± 2	17 ± 2
	d$N(E)$/dE PL	33 ± 4	28 ± 4
	d$N(E)$/dE BL	30 ± 4	26 ± 4
XPS	$N(E)$ P	11 ± 5	11 ± 5
	$N(E)$ AT	15 ± 5	15 ± 5
	$N(E)$ PL	22 ± 10	22 ± 10
	$N(E)$ ATL	30 ± 6	30 ± 6

four methods of evaluation, peak to peak analysis (P), peak to background (B) and then P and B combined with the assumption of single layer adsorption (PL and BL). For the quantitative estimate we use tabulated sensitivity factors [19]. These factors are valid for excitation with 10 kV electrons which we used in the AES experiment. The XPS data are analyzed peak to peak (P) and by the peak areas (A), with and without assuming the single layer status (L). In the case of the area analysis the Tougaard background method [20] has been applied additionally (T).

In Fig. 9 a small region of the $(\sqrt{7}\times\sqrt{7})$ R19.1° structure is shown after applying filtering for suppression of noise. Since the Pd atoms are a priori not identified, two arrangements of the large white objects (S atoms) with respect to the Pd lattice are possible. We show one of those only. The structure of Fig. 9a looks like a structure with two S atoms and weak evidence for Pd atoms in the unit cell. The model (which agrees with Fig. 9a) in Fig. 9b is based on a mixed unit cell containing two S atoms and three Pd atoms (mixed structure).

The atomic position in the different models were checked by FLAPW calculations (fully potential linearized augmented plane waves) using the WIEN97 code [21,22]. The calculations for $(\sqrt{7}\times\sqrt{7})$R19.1° models with one and two S atoms in the unit cell have energetic minima. The $(\sqrt{7}\times\sqrt{7})$R19.1° model with one S atoms is improved when allowing atomic relaxations causing, i.e. the shift of three Pd atoms towards the adsorbate layer in qualitative agreement with the $(\sqrt{7}\times\sqrt{7})$R19.1° structure formed by segregation [8,9]. The two-S-atom structures are energetically favorable in case of mixed structures only. The optimized structure presented in Fig. 9b has one S atom on an fcc and the other on an hcp site. Three Pd atoms are shifted into the adsorbate layer on fcc sites. The three-S-atom structure proposed by Forbes at al. [1] with one S atom on the surface and two S atoms in deeper layers could not be calculated since the unit cell is too large. However, we can exclude this structure simply because of the lower S coverage of 0.28 monolayers in our study compared with 0.43 monolayers [1]. The two-S-atom model proposed agrees qualitatively with the mixed layer models [5,6,8,9]. The EXAFS data [6]

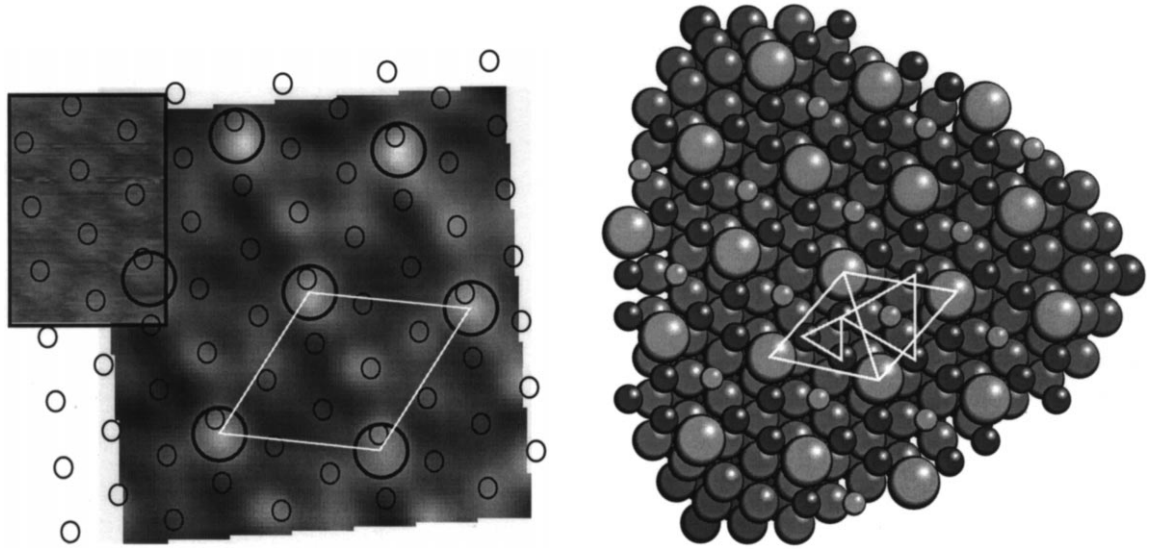

(a) (b)

Fig. 9. (a) Detailed STM topograph of the $(\sqrt{7}\times\sqrt{7})$R19.1° structure. The inset at the upper left shows an STM topograph of the clean Pd(111) structure, which is used to extrapolate the Pd(111) lattice onto the image with the S $(\sqrt{7}\times\sqrt{7})$R19.1°. This is the best achievable fit though not all of the circles exactly hit a protrusion in the STM image. (b) Model of the $(\sqrt{7}\times\sqrt{7})$R19.1° structure based on FLAPW calculations. The orientation is with respect to that in (a).

can exclude essentially any non-mixed adsorbate layers. Further comparison with our work is not possible since Dhanak at al. [6] assume an S coverage of 3/7 monolayers ('known coverage' [1,5]). Consequently, also the$(\sqrt{7}\times\sqrt{7})$R19.1° models based on the analysis by LEED [5,10] are hardly comparable because they are based on a 3/7 monolayer coverage whereas our AES and XPS data are compatible with 2/7 monolayers at most.

5. Summary

The adsorption of H_2S on Pd(111) leads to S adsorption structures which are distinctly different from the S structures produced by segregation. Adsorption from the gas phase results at room temperature in disordered adsorption, $(\sqrt{3}\times\sqrt{3})$R30°, $(\sqrt{7}\times\sqrt{7})$R19.1° and stripes of (2×2) areas. The smooth steps of the clean Pd(111) surface are roughened by the S adsorption. Annealing favors the $(\sqrt{7}\times\sqrt{7})$R19.1° structure. For the $(\sqrt{7}\times\sqrt{7})$R19.1° structure we propose a 'mixed layer' model based on FLAPW calculations. The S segregation produces disordered areas, the $(\sqrt{7}\times\sqrt{7})$R19.1° structure, and triangular 2D islands with a (2×2) structure. The steps of the Pd(111) surface are decorated with stripes of (2×2) ordered S. Extended annealing leads to a dominance of the triangular islands. The growth of the islands is explained using a random walk type of model.

Acknowledgements

This work is supported by the DFG.

References

[1] J.G. Forbes, A.J. Gellmann, J.C. Dunphy, M. Salmeron, Surf. Sci. 279 (1992) 68.
[2] T.M. Gentle, E.L. Mutterties, J. Phys. Chem. 87 (1983) 2469.
[3] D.E. Hunka, T. Picciotto, D.M. Jaramillo, D.P. Land, Surf. Sci. 421 (1999) 166.
[4] F. Maca, M. Scheffler, W. Berndt, Surf. Sci. 160 (1985) 467.
[5] M.E. Grillo, C. Stampfl, W. Berndt, Surf. Sci. 317 (1994) 84.
[6] V.R. Dhanak, A.G. Shard, B.C.C. Cowie, A. Sontoni, Surf. Sci. 410 (1998) 321.
[7] C.H. Patterson, R.M. Lambert, Surf. Sci. 187 (1987) 339.
[8] J. Bömermann, M. Huck, J. Kuntze, T. Rauch, S. Speller, W. Heiland, Surf. Sci. 357–358 (1996) 849.
[9] J. Bömermann, Thesis, Universität Osnabrück, Shaker Verlag, 1998 (ISBN 3-8265-3684-3)
[10] W. Liu, K.A.R. Mitchell, W. Berndt, Surf. Sci. Lett. 393 (1997) L119.
[11] Th. Rauch, Thesis, Universität Osnabrück, 1999 (http://elib.Uni-Osnabrueck.DE/dissertations/physics/T.Rauch/promo.ps.gz)
[12] H. Niehus, Phys. Status Solidi 192 (1995) 357.
[13] E.H. Conrad, H. Hörnis, Progr. Surf. Sci. 48 (1995) 221.
[14] P. Zeppenfeld, M. Krzyzowski, Ch. Romainczyk, G. Comsa, M. Lagally, Phys. Rev. Lett. 72 (1994) 2737.
[15] D. Bürgler, G. Tarrach, T. Schaub, R. Wiesendanger, H.J. Güntherodt, Phys. Rev. B 47 (1993) 9963.
[16] P.J. Feibelmann, D.R. Haman, Surf. Sci. 149 (1985) 48.
[17] N.D. Lang, Phys. Rev. Lett. 56 (1986) 1164.
[18] I.S. Tilinin, M.K. Rose, J.C. Dunphy, M. Salmeron, M.A. van Hove, Surf. Sci. 418 (1998) 511.
[19] L.E. Davis, N.C. MacDonald, P.W. Palmberg, G.E. Riachand, R.E. Weber, Handbook of Auger Electron Spectroscopy, Physical Electronics Industries, Eden Prairie, MN, 1994.
[20] S. Tougaard, J. Vac. Sci. Technol. A 8 (1990) 2197.
[21] P. Blaha, K. Schwarz, J. Luitz, WIEN97, A Full Potential Linearized Augmented Plane Wave Package for Calculating Crystal Properties, 1997
[22] P. Blaha, K. Schwarz, J. Luitz, WIEN97, User's Guide, 1997